# NEUROPLASTIC EXPANSION IN DEEP REINFORCE-MENT LEARNING

**Anonymous authors**Paper under double-blind review

### **ABSTRACT**

The loss of plasticity in learning agents, analogous to the solidification of neural pathways in biological brains, significantly impedes learning and adaptation in reinforcement learning due to its non-stationary nature. To address this fundamental challenge, we propose a novel approach, Neuroplastic Expansion (NE), inspired by cortical expansion in cognitive science. NE maintains learnability and adaptability throughout the entire training process by dynamically growing the network from a smaller initial size to its full dimension. Our method is designed with three key components: (1) elastic topology generation based on potential gradients, (2) dormant neuron pruning to optimize network expressivity, and (3) neuron consolidation via experience review to strike a balance in the plasticitystability dilemma. Extensive experiments demonstrate that NE effectively mitigates plasticity loss and outperforms state-of-the-art methods across various tasks in MuJoCo and DeepMind Control Suite environments. NE enables more adaptive learning in complex, dynamic environments, which represents a crucial step towards transitioning deep reinforcement learning from static, one-time training paradigms to more flexible, continually adapting models.

## 1 Introduction

In the realm of neuroscience, it has been observed that biological agents often experience a diminishing ability to adapt over time, analogous to the gradual solidification of neural pathways in the brain (Livingston, 1966). This phenomenon, typically known as the *loss of plasticity* (Mateos-Aparicio & Rodríguez-Moreno, 2019), significantly affects an agent's capacity to learn continually, especially when agents learn by trial and error in deep reinforcement learning (deep RL) due to the non-stationarity nature. The declining adaptability throughout the learning process can severely hinder the agent's ability to effectively learn and respond to complex or non-stationary scenarios (Abbas et al., 2023). This limitation presents a fundamental obstacle to achieving sustained learning and adaptability in artificial agents, which echoes the *plasticity-stability dilemma* (Abraham & Robins, 2005) observed in biological neural networks.

There have been several recent studies highlighting a significant loss of plasticity in deep RL (Kumar et al., 2020; Lyle et al., 2022), which substantially restricts the agent's ability to learn from subsequent experiences (Lyle et al., 2023; Ma et al., 2023). The identification of primacy bias (Nikishin et al., 2022) further illustrates how agents may become overfitted to early experiences, which inhibits learning from subsequent new data. The consequences of plasticity loss further impede deep RL in continual learning scenarios, where the agent struggles to sequentially learn across a series of different tasks (Dohare et al., 2024).

Research on addressing plasticity loss in deep RL is still in its early stages, with recent approaches including parameter resetting (Nikishin et al., 2022; Sokar et al., 2023) (or its advancement with random head copies (Nikishin et al., 2024)), and several implementation-level techniques like normalization, activation functions, weight clipping, and batch size adjustments (Obando Ceron et al., 2023; Nauman et al., 2024; Elsayed et al., 2024). However, reset-based methods often lead to performance instability and training inefficiency due to the need for period re-training, while implementation-level modifications lack generalizability and do not directly target the plasticity issue. The field currently lacks a unified methodology that can effectively address plasticity loss while maintaining training stability and efficiency across varying environments.

Humans adapt to environmental changes and novel experiences through cortical cortex expansion in cognitive science (Welker, 1990; Hill et al., 2010). This process involves the gradual activation of additional neurons and the formation of new connections to facilitate the ability to learn continually. Drawing inspiration from this biological mechanism, we propose a novel perspective – *Neuroplastic Expansion*, which can help maintain plasticity in deep RL. The key insight is that an agent starting learning with a smaller network and dynamically growing to a larger size (ultimately reaching the original static network dimension) can effectively tackle plasticity loss by maintaining a high level of elastic neurons throughout training (Figure 1). *Elastic neurons means neurons that have plasticity. In this paper, the words elastic and plastic are interchangeably*. We first provide empirical evidence in (§3.1) validating its potential for mitigating plasticity loss and improving final performance in certain cases, even with a naive incremental expansion. We provide a detailed description of plasticity loss and Pruning for RL in Appendix A.

Building upon this insight, we systematically introduce Neuroplastic Expansion (NE), a simple yet effective mechanism to maximize the benefits of incremental growth training (§3.2). (NE) adds highquality elastic candidates based on potential gradients (Evci et al., 2020). However, this will lead to increased computation costs for always enlarging the network, and cannot fully leverage its expressivity as elastic neurons, which are activated and can be updated to fit the new data, may turn dormant during the course of training (Appendix F.8 visualize dormant neurons can diminish representational capacity and leads to suboptimal behavior).

To address this challenge, (NE) introduces a reactivation process for dormant neurons, pruning them and potentially reintroducing them as candidates in subsequent growth stages, thereby better utilizing the network expressivity and enhancing the policy's sustainable learning ability.

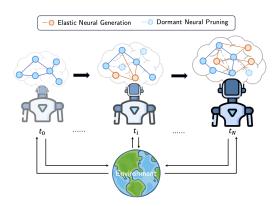


Figure 1: **High-level illustration of Neuroplastic Expansion RL**. The network regenerates elastic neurons based on gradient potential, recycles dormant neurons, and undergoes progressive topology growth to mitigate plasticity loss. The agent consolidates neurons through experience review, preserving prior helpful knowledge and ensuring policy stability.

Unlike previous reset-based approaches (either rest last layers or introducing copies of heads or reinitializing some parts in the network) that risk forgetting and require periodic re-training, NE maintains learning continuity in a smoother way. To further mitigate potential instability from continuous topology adjustments, we introduce an effective Experience Review technique for consolidating neurons by adaptively reviewing prior knowledge during the later training stages to uphold policy stability, striking a balance in the stability-plasticity dilemma. Extensive experiments across long-term training, continual adaptation, and vision RL tasks demonstrate the effectiveness of our method in various scenarios, showcasing our method's ability to maintain plasticity while ensuring policy stability.

The main contributions are summarized as follows:

- We introduce a novel mechanism, *Neuroplastic Expansion* (NE), to mitigate the loss of plasticity in deep RL.
- We develop effective activated neuron generation and dormant neuron pruning mechanism for better network capacity utilization, and a neuron consolidation technique for preventing forgetting helpful reusable knowledge.
- We conduct extensive experiments in standard RL tasks, which demonstrate the effectiveness of NE across various tasks including MuJoCo (Todorov et al., 2012) and DeepMind Control Suite (DMC) (Tassa et al., 2018a) tasks that outperform previous strong baselines by a large margin, and can be effectively adapted to continual learning scenarios.

# 2 BACKGROUND

Deep Reinforcement Learning The reinforcement learning problem can be typically formulated by a Markov decision process (MDP) represented as a tuple  $(\mathcal{S}, \mathcal{A}, \mathcal{P}, \mathcal{R}, \gamma)$ , with  $\mathcal{S}$  denoting the state space,  $\mathcal{A}$  the action space,  $\mathcal{P}$  the transition dynamics:  $\mathcal{S} \times \mathcal{A} \times \mathcal{S} \to [0,1]$ ,  $\mathcal{R}$  the reward function:  $\mathcal{S} \times \mathcal{A} \to \mathbb{R}$ , and  $\gamma \in [0,1)$  the discount factor. The agent interacts with the unknown environment with its policy  $\pi$ , which is a mapping from states to actions, and aims to learn an optimal policy that maximizes the expected discounted long-term reward. The state-action value of s and a under policy  $\pi$  is defined as  $Q^{\pi}(s,a) = \mathbb{E}_{\pi}[\sum_{t=0}^{\infty} \gamma^{t} \mathcal{R}(s_{t},a_{t})|s_{0} = s, a_{0} = a]$ . In actor-critic methods, the actor  $\pi_{\phi}$  and the critic  $Q_{\theta}$  are represented using neural networks as function approximators with parameters  $\phi$  and  $\theta$  (Fujimoto et al., 2018; Haarnoja et al., 2018). The critic network is updated by minimizing the temporal difference loss, i.e.,  $\mathcal{L}_{Q}(\theta) = \mathbb{E}_{D}\left[(Q_{\theta}(s,a) - Q_{\theta}^{T}(s,a))^{2}\right]$ , where  $Q^{T}(s,a)$  denotes the bootstrapping target  $\mathcal{R}(s,a) + \gamma Q_{\bar{\theta}}(s', \pi_{\bar{\phi}}(s'))$  computed using target network parameterized by  $\bar{\phi}$  and  $\bar{\theta}$  based on data sampled from a replay buffer D. The actor network  $\phi$  is typically updated to maximize the Q-function approximation according to  $\nabla_{\phi}J(\phi) = \mathbb{E}_{D}\left[\nabla_{a}Q_{\theta}(s,a)|_{a=\pi_{\phi}(s)}\nabla_{\phi}\pi_{\phi}(s)\right]$ .

Activated Neuron Ratio Activated neurons are found to be updated by new data easily. So the proportion of activated neurons in the network, i.e. activated neuron ratio, is often thought to be positively correlated with plasticity Ma et al. (2023). It is defined as those whose output is beyond a certain threshold  $\tau$  in the neural network, That is, count the number of neurons other than dormant neurons (Xu et al., 2023). Formally, a neuron i in layer l is considered activated when  $f(l_i) > \tau$  which are opposed to dormant neurons (Sokar et al., 2023), where

$$f(l_i) = \frac{\mathbb{E}_{x \in Id} |h_i^l(x)|}{\frac{1}{H^l} \sum_{k \in h} \mathbb{E}_{x \in Id} |h_k^l(x)|},$$
(1)

with *Id* denoting the input distribution. The relationship between the Activated Neuron Ratio curve and plasticity is: The primary cause behind an agent's plasticity loss is the rapid dormancy of numerous neurons as training progresses, diminishing the model's representational capacity (Sokar et al., 2023; Qin et al.). Consequently, postponing the reduction in activated neurons is commonly viewed as a means to alleviate plasticity loss, i.e. the downward trend of the curve. Activated neuron ratio is widely used in plasticity visualization (Ma et al., 2023) due to its intuitive interpretation.

# 3 NEUROPLASTIC EXPANSION RL

In this section, we begin by discussing the insights of Neuroplastic Expansion RL empirically, and analyze its effect on mitigating loss of plasticity in Section 3.1. Then, we systematically present details of our method in Section 3.2.

#### 3.1 ILLUSTRATION OF INSIGHTS OF DYNAMIC GROWING RL

There have been several recent studies investigating loss of plasticity in supervised learning (Lyle et al., 2023; Lewandowski et al., 2024), which corresponds to the phenomenon where neural networks gradually lose the ability to adapt and learn from new experiences (Lin et al., 2022). This is further exacerbated in RL (Sokar et al., 2023; Nikishin et al., 2024), due to the non-stationary nature and the tendency to overfit prior knowledge, resulting in suboptimal policies. A predominant approach to tackle plasticity loss is based on resetting (Nikishin et al., 2022), where the agent resets the last few layers of its neural network periodically throughout training. However, although effective, this kind of approach typically forgets helpful and reusable knowledge which is critical for learning, and thus the agent experiences a drop in performance once resetting is applied.

A major causes for agents to adapt to novel circumstances is based on the growth of the human cortex (Hill et al., 2010). Motivated by this insight, we propose a novel perspective that RL agents can maintain high plasticity through dynamic neural expansion mechanisms, sustaining the policy's continual adaptation ability from new experiences. Initially, data collected by a random policy may be of lower quality and therefore require less network expressivity to fit (Burda et al., 2018; Zhelo et al., 2018). As the agent improves, it tends to need a more expressive network for fitting the more

complex value estimates and policies. Maintaining neuronal vitality and regeneration during training can significantly mitigate plasticity loss, as it allows for ongoing adaptation to new information.

Motivated by this insight, we propose a novel angle considering Neuroplastic Expansion, where the agent starts with a smaller network that evolves to a larger one throughout the learning process. We first demonstrate a naive implementation of this idea and will systematically discuss our methodology in Section 3.2. Concretely, we consider a small-to-large neural expansion approach, where the capacity of initial networks is 20% of the size of a typical full TD3 (Fujimoto et al., 2018) network (i.e., uniformly selected 20% of neurons from each layer in the full TD3). To validate the potential of this novel perspective, we first consider the simplest manner for growing the network by uniformly adding k new connections in the current critic topology  $\dot{\theta} \subset \theta$ 

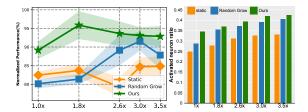


Figure 2: Comparison of normalized performance (left) and the ratio of active neurons (right) for vanilla TD3 (Fujimoto et al., 2018) and its variant with a naive random growth network and our *Neuroplastic Expansion* method, across varying network capacities. Results for uniform fine-grained size sampling are in the Appendix F.10. Results for uniform fine-grained setting sizes are in the AppendixExperiments are conducted with 7 independent seeds.

and current actor topology  $\check{\phi} \subset \phi$  for each layer  $l \in N$  and participate in gradient propagation according to  $\mathbb{I}_{grow} = \operatorname{Random}_{i \notin \check{\phi}_l}(\theta_l, k) \cup \operatorname{Random}_{i \notin \check{\phi}_l}(\phi_l, k)$ .

We build this idea upon TD3 and conduct fair comparisons with vanilla TD3 (i.e., with static actor and critic networks) with different capacities. We compared the performance of the dynamic growing network with a naive topology growth strategy, with the typical ones using static networks based on TD3 (Fujimoto et al., 2018) in the HalfCheetah environment. The final network size of NE is the same as that of the other methods to ensure comparing fairness. Therefore, the comparison with the vanilla TD3 algorithm is fair given the same network capacity at the end of training.

From the left part in Figure 2, we observe that even a naive incremental network growth can bring relatively noticeable gains to the agent considering larger network capacity. The right part in Figure 2 demonstrates the ratio of active neurons (Sokar et al., 2023) for each algorithm during training. This metric is used to evaluate RL agents regarding whether they maintain expressive ability. As shown, topology growth can effectively alleviate neuron deactivation and thus maintain the ability of policy learning to mitigate the loss of plasticity and alleviate the primacy bias.

#### 3.2 METHOD: NEUROPLASTIC EXPANSION

Hill et al. (2010) demonstrated that the cerebral cortex undergoes expansion in response to environmental stimuli, learning, and novel experiences. This dynamic growth and reorganization enhances cognitive and decision-making abilities, fostering adaptability to changing situations. Motivated by our preliminary results and inspired by this biological mechanism, we present *Neuroplastic Expansion* (NE), which trains RL agents with a dynamic expansion network and seeks to maintain the ability to retain learning capacity and adaptability throughout the entire learning cycle.

Elastic Topology Generation While incremental random topology growth has contributed to maintaining plasticity, we aim to elucidate the underlying mechanisms that drive its effectiveness. We pursue this goal by delving into the dormant neuron theory (Sokar et al., 2023), a prevalent explanation for plasticity loss currently. This theory posits that neurons within a network become inactive during training, generally measured by their activations going to zero (Lu et al., 2019). This hinders said neurons' ability to learn, reducing the network's overall ability to efficiently process new situations and the outputs gradually diminish, ultimately dropping below the activation function threshold (Lu et al., 2019). Meanwhile, another line of work revealed that parameters lacking prompt exposure to high-gradient stimuli are prone to slipping into dormancy. Drawing from the aforementioned findings, we derive the following observation:

The naive random topology growth sporadically introduces new connections that can generate significant gradients for neurons nearing dormancy, thereby supplying them with potent signals during backpropagation and continue learning.

If the above conjecture aligns with the underlying principles in deep RL, choosing topology candidates based on the gradient magnitude could alleviate plasticity loss more effectively than randomly expanding the network connections. To this end, we follow the sparse network training framework in Tan et al. (2022). Prior to each topology expansion, a batch of transitions is sampled from buffer D

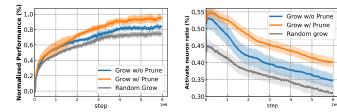


Figure 3: **Performance comparison and plasticity evaluation of random growth**, our proposed growth method, and pruning mechanisms. All experiments run with seven independent seeds.

to compute the magnitude of gradient through the whole model parameters, formalized as  $|\nabla_{\theta}L|$ . Then k connections capable of yielding the highest magnitude are chosen to augment the topology:  $\mathbb{I}_{grow} = ArgTopk_{i\notin\theta^l}(|\nabla_{\theta}^lL|)$ . The topology growing process  $G_k$  adaptively starts every  $\Delta T$  step. We try several growing schedules to achieve warm topology growth to prevent training instability caused by significant network modifications. Finally, we chose cosine annealing through practice (see Appendix F.6 for experiments): at timestep t the k is decayed in a cosine annealing manner:  $\frac{\alpha}{2}(1+\cos(\frac{t\pi}{Topd}))$ , where  $\alpha$  denotes the discount factor and  $T_{end}$  is the shut down step.

The results depicted in Figure 3 indicate that substituting random growth with the selection of new connections based on potentially provided gradients can enhance the agent's performance and mitigate the dormant neuron issue. Furthermore, we compare two commonly used topology initial strategies: uniform and Erdos-Rrenyi (Evci et al., 2020), and we find that initializing the network in Erdos-Rrenyi type is slightly more effective for RL. Erdos-Rrenyi enables the number of connections in a sparse layer to scale with the sum of the number of output and input channels, which in turn ensures more stable computations in small networks. Furthermore, the agent can also perform more efficient learning in the early stage. In Appendix E, we explain why we use the total network to calculate the gradients instead evaluating weights one-by-one.

**Dormant Neuron Pruning** After replacing the naive growth with our gradient guidance growing process  $G_k$ , a new challenge emerges, i.e., dormant neurons exhibit a stark decline in their representational potency while tenaciously occupying network capacity. Such inactive neurons could be inherent from the initialization or introduced into the network topology through the growth schedule. This situation may lead to a topology that saturates quickly with disproportionately small computational power. Moreover, Lu et al. (2019); Liu et al. (2019) demonstrated that parameters solely forward-linked to dormant neurons are omitted from the gradient calculation process, rendering them ineffective as they fail to receive meaningful guidance signals. We hypothesize that pruning and resetting of dormant neurons following the growth of the topology could address this issue.

This process aims to free up space for new connections, reactivating dormant neurons as new candidates. According to (Ceron et al., 2024a;b), sparsifying the value-based agents' network can often enhance the performance, which offers assurance for our real-time pruning empirically. Consequently, we introduce a synchronous dormant neuron prune-and-reset mechanism into the topology growth schedule  $G_k$ . Here, we adopt the calculation method  $f(\cdot)$  showed in Eq.1 and set  $\tau$  to be 0, which means only considering fully dormant neurons:  $\mathbb{I}_{prune} = \{ \mathrm{index}(\theta_i) | f(\theta_i) = 0 \}$ . To facilitate the topology's gradual growth and avoid over-pruning, we use  $Clip(0, |\mathbb{I}^l_{prune}|, \omega \times |\mathbb{I}^l_{grow}|)$  to clip the prune number in to range  $[0, \omega \times |\mathbb{I}^l_{grow}|]$ , where  $|\mathbb{I}^l_{grow}|$  and  $|\mathbb{I}^l_{prune}|$  are real numbers denote the number of elements in  $\mathbb{I}^l_{grow}$  and  $\mathbb{I}^l_{prun}$  separately. The parameter  $\omega$  is a preset ratio parameter  $0 \le \omega < 1$  that applies a "discount" factor to the total growth in layer l. When the size of the pruning set exceeds this upper limit, elements are randomly removed from  $\mathbb{I}^l_{prune}$  until the constraint is satisfied. The Clip function takes the form  $Clip(\min$  value, input, max value), where min value represents the lower bound, and input represents the value to be numerically restricted, max value is the upper bound of the allowed range (please refer to Appendix D.2 for the pseudocode). Therefore,

the final two parameters that control topology change are k and  $\omega$  so we will use  $G_{k,\omega}$  to refer to our whole grow-prune schedule. The complete growth-pruning schedule for each layer l in actor  $\phi$  and critic  $\theta$  can be rewritten as

$$G_{k,\omega}: \left\{ \begin{array}{l} 1. \ \mathbb{I}^{l}_{grow} = ArgTopk_{i\notin \check{\phi}^{l}}(|\nabla^{l}_{\phi}L^{\phi}_{t}|) \cup ArgTopk_{i\notin \check{\theta}^{l}}(|\nabla^{l}_{\theta}L^{\theta}_{t}|) \\ 2. \ \mathbb{I}^{l}_{prune} = \left\{ \operatorname{Index}(\check{\phi}^{l}_{i})|f(\check{\phi}^{l}_{i}) = 0 \right\} \cup \left\{ \operatorname{Index}(\check{\theta}^{l}_{i})|f(\check{\theta}^{l}_{i}) = 0 \right\}; \end{array} \right. \tag{2}$$

We then use  $\mathbb{I}^l_{grow}, \mathbb{I}^l_{prune}$  to generate  $\{0,1\}$  masks and dot multiply the network parameters to achieve the evolution of the actor topology  $\check{\phi}$  and critic topology  $\check{\theta}$ . The results in Figure 3 show that with the addition of the pruning mechanism after each growth round, the plasticity of the RL network is further preserved and the performance is further improved. Compared with plasticity injection (PI), although both NE and PI maintain plasticity by extending networks, PI only focuses on one-time large-scale growth of the network, while our method employs finer-grained topology level growth and pruning to achieve real-time warm network change.

Notably, our sparse network training framework for maintaining the stable learning is summarized from above as: (i) Inspired by (Evci et al., 2020), we use Erdos-Rrenyi initialization to make the number of connections in a sparse layer to scale with the sum of the number of output and input channel for ensuring the start stability. (ii) We employs cosine annealing to guide the warm growth to reduce the noise caused by network change. (iii) Following the sparse training in RL (Tan et al., 2022), the first and last layers are dense to ensure the stability of the encoding and decoding.

Neuron Consolidation via Experience Review As discussed above, the proposed elastic topology generation and dormant neuron pruning-based dynamic growing approach can greatly mitigate plasticity loss. This approach smoothly maintains a higher level of active neurons, leading to improved performance. However, a more careful investigation of the results, i.e. Tab.8, shows that NE demonstrate high standard deviation across seeds in the later stage of

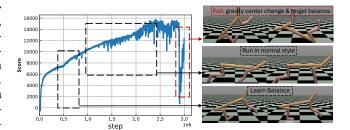


Figure 4: Instability of NE without neuron consolidation via experience review at the later stage.

training which reveals that there is a potential risk of performance oscillation near convergence. We hypothesize that this is because high-frequency changes in the network topology may cause slight probability errors in the network topology changes. As a result, with the activated neuron ratio decrease, some agents could run the risk of forgetting skills learned in the initial stage (e.g., standing in halfcheetah), leading to differentiated suboptimal behavior after convergence and a higher standard deviation between seeds.

We examined the behavior of all seeds on the HalfCheetah task and found that there are multiple runs in which the agent no longer had the ability to stand after a fall (Figure 4). This insight enhancees our confidence to the above conjecture. To this end, we hope to find a topology-agnostic and simple technique to further enhance the stability of NE by mitigating catastrophic forgetting. Meanwhile, (Rolnick et al., 2019; Zhou et al., 2020) find that experience replay (ER) exhibit properties of mitigating forgetting and using it to maintain network plasticity in RL and supervised learning. Inspired by these works, we hope to build an ER mechanism that sensitive to the training stage and activated neuron ratio.

In practice, we consider the absolute slope of activated neuron ratio curve  $\Delta(f(\theta)) := \sum_{i \in \theta} |\Delta f(\theta_i)|$  as the threshold  $\epsilon$ . Specifically,  $\epsilon$  measures the slope of changes in the number of activated neurons (within the critic network) during the recent c steps, i.e., [150, 450]. A larger positive value of  $\epsilon$  corresponds to a relatively greater reduction of dormant neurons from our proposed dynamic growing network, while a small value of  $\epsilon$  close to zero indicates a bottleneck in improved plasticity gains, which also indicates a limited space for further topology expansion and marks the later stage of policy learning (Figure 5). We generally observe that  $\epsilon$  decreases during the course of training, as elastic neuron generation and dormant neuron pruning will lead to a larger change in the number of dormant neurons in the early stage (and cannot always enlarge the proportion of active

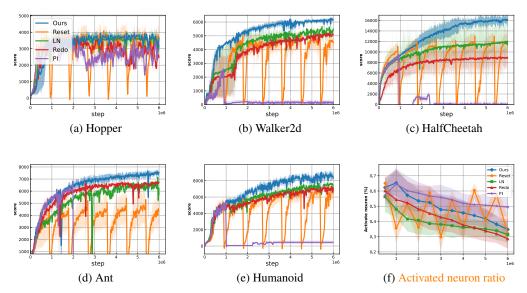


Figure 6: Performance comparisons on OpenAI MuJoCo environments (Todorov et al., 2012) (a) Hopper (b) Walker2D (c) HalfCheetah (d) Ant (e) Humanoid. (f) Results of the activated neurons ratio. Our method outperforms baselines in all four tasks and maintains high activate neurons ratio.

neurons due to limited network capacity). We encourage the agent to review earlier experiences in the buffer when there are more dormant neurons. At each training step, a random number  $m \in [0,1]$  is selected, if  $m > \epsilon$ , the sampling is conducted from the initial quarter of the buffer; otherwise, the conventional sampling method is employed. We use pseudocode to make the whole process of the algorithm clear in Appendix D.1

#### 4 EXPERIMENTS

In this section, we conduct comprehensive experiments to evaluate whether NE can alleviate the loss of plasticity. We investigate the following key questions: (i (§4.1)) On long-term training setting, can NE effectively combat early data overfitting, enhance performance, and attenuate the decline in activation neuron ratio? (ii (§4.2)) In continuous adaptation task, can NE enable agents to adapt to new tasks efficiently and slow down the activation neuron dormancy speed without being constrained by prior learning limitations (iii (§4.3)) What are the effects of NE on the policy and value network and the importance of different components? (iv (§4.4)) Can our method be applied to other deep RL methods with more complex image inputs?

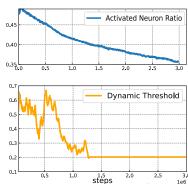


Figure 5: How  $\epsilon$  changes with plasticity measurement. In practice, we set a lower bound for  $\epsilon$ .

#### 4.1 Long-term Training Tasks

Experimental Setup We first conduct a series of experiments based on the standard continuous control tasks on OpenAI Gym (Brockman, 2016) simulated by MuJoCo (Todorov et al., 2012) with long-term training setting, i.e. 3M steps → 6M. We compare NE against strong baselines including Reset (Nikishin et al., 2022), ReDo (Sokar et al., 2023), Layer Normalization (LN) (Lyle et al., 2024b), and Plasticity Injection (PI) (Nikishin et al., 2024). To mitigate implementation bias and ensure a fair comparison, all baselines are implemented based on official implementations (Sokar et al., 2023; Nikishin et al., 2024; 2022), with the same architecture (See Appendix C.1). We build all baselines based on the popular TD3 (Fujimoto et al., 2018) algorithm (where results based on other backbone deep RL methods are discussed in Section 4.4). For each algorithm we run 14 seeds

and report the mean and standard deviation. A detailed description of the hyperparameters and setup can be found in Appendix C.2. The growth termination scale for NE is set to match that of the baselines. For all tasks, NE initializes agents from 25% of total capacity and grows asymptotically. The score in all figures denotes the undiscounted episodic return.

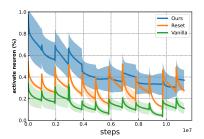
Results As shown in Figure 6, Reset inevitably suffers from periodic sharp performance drops after each reset for reviving dormant neurons to a large extent, as it can lead to the loss of reusable knowledge that necessitates relearning and impedes the overall progress. LN and ReDo demonstrate more stable performance compared to Reset, but result in a lower proportion of active neurons, while PI maintains the highest level of neuron activation, but only performs in the relatively easier Hopper environment. Our method achieves significant and consistent performance improvements compared to these strong recent baselines in terms of learning efficiency and final performance, with a larger margin in more complex environments. In addition, it effectively improves the loss of plasticity as it maintains a higher level of active neuron ratio throughout training compared to the most competitive LN method. It also better trade-off between performance and neuron utilization, as it performs stably and achieves better performance than PI, which has the highest neuron activation but suboptimal performance in most tasks.

#### 4.2 CONTINUAL ADAPTATION

In this section, we investigate the continual ability to learn and adapt to changing environments, which is a key ability of deep RL agents (Abbas et al., 2023; Elsayed & Mahmood, 2024).

Experimental Setup We follow the experimental paradigm of Abbas et al. (2023), and evaluate our proposed method on a variant of MuJoCo tasks that involve non-stationarity due to changing environments over time. Specifically, the agent is trained to master a sequence of 4 environments (HalfCheetah  $\rightarrow$  Humanoid  $\rightarrow$  Ant  $\rightarrow$ Hopper), starting with HalfCheetah for 1000 episodes of training, followed by the next task for the same number of episodes. A cycle is completed when training on Hopper is finished. The agent revisits this sequence of environments three times, constituting a long-term training schedule. Each task maintains an output head (1 layer MLP), which is trained in conjunction with the backbone network. Our method is applied to the layers excluding the output head. We compare our approach with the vanilla TD3 agent and the most competitive baseline, Reset (re-initialize network when task is changed), which breaks the setting constraint to simplify the process to single-task learning. (Abbas et al., 2023).

**Results** The performance of each method for a single environment when repeatedly learning on a sequence of environments as described above is summarized in Figure 8. We aim to evaluate (i) the efficiency of the policy in swiftly learning the subsequent task after mastering the previous one within a single cycle, (ii) the agent's ability to retain the benefits of initial learning for the same task across multiple cycles. As shown, Resetting, which involves initializing the parameters after each task, is currently deemed the most effective approach.



According to the row in Figure 8, NE adeptly handles each task without being influenced by previous training. It significantly outperforms the original TD3, emphasizing that standard RL algorithms do suffer from catastrophic for-

Figure 7: Activated neuron ratio, id recorded for three agents with different settings during cyclic training.

getting in the continual learning setting. We attribute this success to NE's capacity to introduce real-time topology adjustments for storing new knowledge, thereby ensuring continuous learning capabilities.

Remarkably, in certain environments, such as Ant, NE-TD3 can retain previous knowledge and seamlessly continue learning. This could be attributed to the experience review module and the preservation of old neurons in the topology, which store pertinent information crucial for successful continual learning. When considering the column-wise comparisons, our method performs comparably to reset in the majority of tasks, yet significantly outshines reset in the challenging Humanoid

environment. The comparison in terms of active neurons for each baseline is shown in Figure 7, which illustrates that even in the long training schedule, NE can effectively alleviate neuron dormancy while efficiently learning, and it even performs better than resetting all parameters during the early training period.

The spike phenomenon in 7 is related to researches which analysis relationship between input distribution and plasticity, (Lu et al., 2019) obvious that that neurons which fail to activate the activation function can be reactivated when the input distribution to the network is changed. A similar phenomenon has been evident in (Ma et al., 2023) that data augmentation can alleviate the decrease of activated neurons. In the continuous adaptation task we tested, a sudden change in the environment also caused a change in the input data distribution that increased the activated neuron rate, but after a short training period, the neurons went back to dormant.

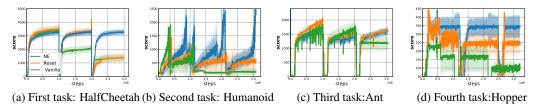


Figure 8: Learning curves of three methods (NE, Reset, Vanilla) on continuous adaptation tasks.

### 4.3 ABLATION STUDY.

In this section, we conduct an additional ablation study to investigate the effectiveness of neuron consolidation in Neuroplastic Expansion, while the importance of elastic neural generation and dormant neural pruning has been demonstrated in Figure 3. We also examine the experience review (ER) module and the impact of our method on the policy and value networks.

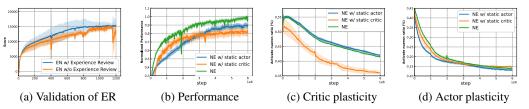


Figure 9: Ablation study: (a) shows the validity verification of ER, while (b) to (d) detail the impact of NE on the actor and critic from the perspectives of plasticity and performance.

As illustrated in Figure 9a, the results on HalfCheetah show ER improves the training stability, particularly in the later stage. Further, we select 4 complex tasks with image input and sparse reward setting to further verify the effectiveness of ER. The results in Appendix F.5 show that when assisted with ER, our training framework always stabilizes the convergent policy at SOTA level across different seeds (lower standard deviation). In contrast, the absence of this critical component leaves the model vulnerable to potential policy collapse in subsequent stages (albeit slighter compared to Reset), demonstrating the critical role of reviewing historical knowledge in maintaining policy stability and preventing the loss of early valuable information as discussed in Section 3.2.

Figure 9b illustrates the comparison result of our method and its variants, isolating the effects of NE on the actor and critic networks separately. We observe that NE is particularly crucial for the critic network. Removing this from the critic leads to significant performance degradation and significant loss of plasticity compared to the full version of NE (Figure 9c,9d); whereas limiting the expansion to only the critic results in a less pronounced drop in performance. This asymmetry in impact may be attributed to the more challenging task faced by the critic, as it needs to provide accurate value estimates for different state-action pairs (Meng et al., 2021) considering a non-stationary data distribution. In addition, the critic also provides guidance signals to actor optimization, which requires high level of adaptability (Fujimoto et al., 2024).

In addition, we analyze in detail whether there is further improvement after combining NE with previous mitigation plasticity methods and empirically analyze the sensitivity of NE to growth rate, replay ratio and initial sparsity in the appendix F.

#### 4.4 VERSATILITY

In this section, we demonstrate the generality of our proposed method by applying it to another popular deep RL method and evaluating its performance on more complex tasks with image input.

**Experimental Setup** We evaluate four image-based motion control tasks from the DeepMind Control Suite (DMC) (Tassa et al., 2018b): Reacher hard, Reacher easy, Walker walk and Cartpole Swingup Sparse, to demostrate the generalization of NE for deep RL algorithms and its robustness across diverse tasks. We consider DrQ (Yarats et al., 2022), a well-known variant of SAC (Haarnoja et al., 2018) specifically designed for processing image inputs, as the backbone algorithm. We use the same baselines from Section 4.1 for comparison.

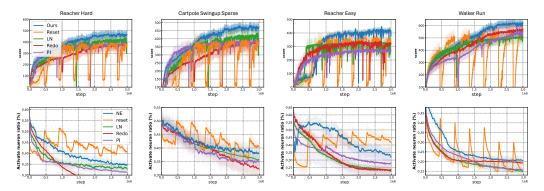


Figure 10: First row shows the performance of five methods. Second row corresponds to the percentage of activated neurons. All experiments run with seven independent seeds

**Results** First row of Figure 10 shows that NE can be effectively combined with DrQ to achieve stable performance on image input tasks, outperforming other baselines in all tasks and demonstrating its versatility across different algorithms. In addition, the second row of Figure 10 (activated neuron ratio) indicates that, although EN cannot reach the peak value set by Reset, it can better delay the dormancy of neurons compared to other warm mitigation strategies and ensure stable performance.

### 5 CONCLUSION

Inspired by the cortical growth in biological agents that triggers neuronal topology expansion to enhance plasticity and adaptability to new situations, we present a novel perspective for deep RL agents to mitigate the loss of plasticity with a dynamic growing network. Building on this insight, we introduce a comprehensive topology growth framework, Neuroplastic Expansion (NE), which addresses both growth and pruning perspectives to maximize the performance benefits of topology expansion. NE adds high-quality elastic neurons and connections based on the gradient to improve the network's learning ability; prunes dormant neurons in a timely manner for better utilizing network capacity, and returns them to the candidate set to maintain the agent's plasticity, making dormant neurons reusable. NE outperforms previous methods which aimed at alleviating plasticity loss on diverse tasks and demonstrates stable, outstanding performance on plasticity metrics. Interesting future directions include the exploration of adaptive architectures that dynamically adjust their capacity based on the agent's performance or task complexity, and further minimizing computational overhead. Overall, despite the acknowledged limitations, our research provides practical insights into enhancing the plasticity of RL agents. We hope our findings pave the way for diverse future explorations, potentially leading to more sample- and parameter-efficient, as well as adaptable, deep RL algorithms.

### REFERENCES

- Zaheer Abbas, Rosie Zhao, Joseph Modayil, Adam White, and Marlos C Machado. Loss of plasticity in continual deep reinforcement learning. In *Conference on Lifelong Learning Agents*, pp. 620–636. PMLR, 2023.
- Wickliffe C Abraham and Anthony Robins. Memory retention—the synaptic stability versus plasticity dilemma. *Trends in neurosciences*, 28(2):73–78, 2005.
- Jordan T. Ash and Ryan P. Adams. On warm-starting neural network training. In *Proceedings of the 34th International Conference on Neural Information Processing Systems*, NIPS '20, Red Hook, NY, USA, 2020. Curran Associates Inc. ISBN 9781713829546.
- Tudor Berariu, Wojciech M. Czarnecki, Soham De, Jörg Bornschein, Samuel L. Smith, Razvan Pascanu, and Claudia Clopath. A study on the plasticity of neural networks. *ArXiv*, abs/2106.00042, 2021. URL https://api.semanticscholar.org/CorpusID:235266002.
- G Brockman. Openai gym. arXiv preprint arXiv:1606.01540, 2016.
- Yuri Burda, Harrison Edwards, Amos Storkey, and Oleg Klimov. Exploration by random network distillation. *arXiv preprint arXiv:1810.12894*, 2018.
- Johan Samir Obando Ceron, Aaron Courville, and Pablo Samuel Castro. In value-based deep reinforcement learning, a pruned network is a good network. In *Forty-first International Conference on Machine Learning*, 2024a. URL https://openreview.net/forum?id=seo9V9QRZp.
- Johan Samir Obando Ceron, Ghada Sokar, Timon Willi, Clare Lyle, Jesse Farebrother, Jakob Nicolaus Foerster, Gintare Karolina Dziugaite, Doina Precup, and Pablo Samuel Castro. Mixtures of experts unlock parameter scaling for deep RL. In *Forty-first International Conference on Machine Learning*, 2024b. URL https://openreview.net/forum?id=X9VMhfFxwn.
- Shibhansh Dohare, J Fernando Hernandez-Garcia, Qingfeng Lan, Parash Rahman, A Rupam Mahmood, and Richard S Sutton. Loss of plasticity in deep continual learning. *Nature*, 632(8026): 768–774, 2024.
- Mohamed Elsayed and A Rupam Mahmood. Addressing loss of plasticity and catastrophic forgetting in continual learning. *arXiv* preprint arXiv:2404.00781, 2024.
- Mohamed Elsayed, Qingfeng Lan, Clare Lyle, and A Rupam Mahmood. Weight clipping for deep continual and reinforcement learning. *arXiv preprint arXiv:2407.01704*, 2024.
- Utku Evci, Trevor Gale, Jacob Menick, Pablo Samuel Castro, and Erich Elsen. Rigging the lottery: Making all tickets winners. In *International conference on machine learning*, pp. 2943–2952. PMLR, 2020.
- Scott Fujimoto, Herke Hoof, and David Meger. Addressing function approximation error in actor-critic methods. In *International conference on machine learning*, pp. 1587–1596. PMLR, 2018.
- Scott Fujimoto, Wei-Di Chang, Edward Smith, Shixiang Shane Gu, Doina Precup, and David Meger. For sale: State-action representation learning for deep reinforcement learning. *Advances in Neural Information Processing Systems*, 36, 2024.
- Laura Graesser, Utku Evci, Erich Elsen, and Pablo Samuel Castro. The state of sparse training in deep reinforcement learning. In *International Conference on Machine Learning*, pp. 7766–7792. PMLR, 2022.
- Tuomas Haarnoja, Aurick Zhou, Pieter Abbeel, and Sergey Levine. Soft actor-critic: Off-policy maximum entropy deep reinforcement learning with a stochastic actor. In *International conference on machine learning*, pp. 1861–1870. PMLR, 2018.
- Jason Hill, Terrie Inder, Jeffrey Neil, Donna Dierker, John Harwell, and David Van Essen. Similar patterns of cortical expansion during human development and evolution. *Proceedings of the National Academy of Sciences*, 107(29):13135–13140, 2010.

- Diederik P Kingma. Adam: A method for stochastic optimization. arXiv preprint arXiv:1412.6980,
   2014.
  - Aviral Kumar, Rishabh Agarwal, Dibya Ghosh, and Sergey Levine. Implicit under-parameterization inhibits data-efficient deep reinforcement learning. *arXiv* preprint arXiv:2010.14498, 2020.
  - Saurabh Kumar, Henrik Marklund, and Benjamin Van Roy. Maintaining plasticity via regenerative regularization. *arXiv preprint arXiv:2308.11958*, 2023.
  - Hojoon Lee, Hanseul Cho, Hyunseung Kim, Daehoon Gwak, Joonkee Kim, Jaegul Choo, Se-Young Yun, and Chulhee Yun. Plastic: Improving input and label plasticity for sample efficient reinforcement learning. In *Neural Information Processing Systems*, 2023. URL https://api.semanticscholar.org/CorpusID:259203876.
  - Hojoon Lee, Hyeonseo Cho, Hyunseung Kim, Donghu Kim, Dugki Min, Jaegul Choo, and Clare Lyle. Slow and steady wins the race: Maintaining plasticity with hare and tortoise networks. *ArXiv*, abs/2406.02596, 2024. URL https://api.semanticscholar.org/CorpusID:270258586.
  - Alex Lewandowski, Haruto Tanaka, Dale Schuurmans, and Marlos C. Machado. Directions of curvature as an explanation for loss of plasticity, 2024. URL https://arxiv.org/abs/2312.00246.
  - TP Lillicrap. Continuous control with deep reinforcement learning. *arXiv preprint* arXiv:1509.02971, 2015.
  - Guoliang Lin, Hanlu Chu, and Hanjiang Lai. Towards better plasticity-stability trade-off in incremental learning: A simple linear connector. In *Proceedings of the IEEE/CVF Conference on Computer Vision and Pattern Recognition*, pp. 89–98, 2022.
  - Yang Liu, Jianpeng Zhang, Chao Gao, Jinghua Qu, and Lixin Ji. Natural-logarithm-rectified activation function in convolutional neural networks. In 2019 IEEE 5th International Conference on Computer and Communications (ICCC), pp. 2000–2008. IEEE, 2019.
  - Robert B Livingston. Brain mechanisms in conditioning and learning. Technical report, 1966.
  - Dor Livne and Kobi Cohen. Pops: Policy pruning and shrinking for deep reinforcement learning. *IEEE Journal of Selected Topics in Signal Processing*, 14(4):789–801, 2020.
  - Lu Lu, Yeonjong Shin, Yanhui Su, and George Em Karniadakis. Dying relu and initialization: Theory and numerical examples. *arXiv preprint arXiv:1903.06733*, 2019.
  - Clare Lyle, Mark Rowland, and Will Dabney. Understanding and preventing capacity loss in reinforcement learning. *arXiv preprint arXiv:2204.09560*, 2022.
  - Clare Lyle, Zeyu Zheng, Evgenii Nikishin, Bernardo Avila Pires, Razvan Pascanu, and Will Dabney. Understanding plasticity in neural networks. In *International Conference on Machine Learning*, pp. 23190–23211. PMLR, 2023.
  - Clare Lyle, Zeyu Zheng, Khimya Khetarpal, James Martens, H. V. Hasselt, Razvan Pascanu, and Will Dabney. Normalization and effective learning rates in reinforcement learning. *ArXiv*, abs/2407.01800, 2024a. URL https://api.semanticscholar.org/CorpusID: 270878053.
  - Clare Lyle, Zeyu Zheng, Khimya Khetarpal, Hado van Hasselt, Razvan Pascanu, James Martens, and Will Dabney. Disentangling the causes of plasticity loss in neural networks. *arXiv preprint arXiv:2402.18762*, 2024b.
  - Guozheng Ma, Lu Li, Sen Zhang, Zixuan Liu, Zhen Wang, Yixin Chen, Li Shen, Xueqian Wang, and Dacheng Tao. Revisiting plasticity in visual reinforcement learning: Data, modules and training stages. *arXiv preprint arXiv:2310.07418*, 2023.
    - Pedro Mateos-Aparicio and Antonio Rodríguez-Moreno. The impact of studying brain plasticity. *Frontiers in cellular neuroscience*, 13:66, 2019.

- Lingheng Meng, Rob Gorbet, and Dana Kulić. The effect of multi-step methods on overestimation in deep reinforcement learning. In 2020 25th International Conference on Pattern Recognition (ICPR), pp. 347–353. IEEE, 2021.
- Michal Nauman, Michał Bortkiewicz, Mateusz Ostaszewski, Piotr Miłoś, Tomasz Trzciński, and Marek Cygan. Overestimation, overfitting, and plasticity in actor-critic: the bitter lesson of reinforcement learning. *arXiv preprint arXiv:2403.00514*, 2024.
- Evgenii Nikishin, Max Schwarzer, Pierluca D'Oro, Pierre-Luc Bacon, and Aaron Courville. The primacy bias in deep reinforcement learning. In Kamalika Chaudhuri, Stefanie Jegelka, Le Song, Csaba Szepesvari, Gang Niu, and Sivan Sabato (eds.), *Proceedings of the 39th International Conference on Machine Learning*, volume 162 of *Proceedings of Machine Learning Research*, pp. 16828–16847. PMLR, 17–23 Jul 2022. URL https://proceedings.mlr.press/v162/nikishin22a.html.
- Evgenii Nikishin, Junhyuk Oh, Georg Ostrovski, Clare Lyle, Razvan Pascanu, Will Dabney, and André Barreto. Deep reinforcement learning with plasticity injection. *Advances in Neural Information Processing Systems*, 36, 2024.
- Johan Obando Ceron, Marc Bellemare, and Pablo Samuel Castro. Small batch deep reinforcement learning. In A. Oh, T. Naumann, A. Globerson, K. Saenko, M. Hardt, and S. Levine (eds.), Advances in Neural Information Processing Systems, volume 36, pp. 26003–26024. Curran Associates, Inc., 2023. URL https://proceedings.neurips.cc/paper\_files/paper/2023/file/528388flad3a481249a97cbb698d2fe6-Paper-Conference.pdf.
- Haoyuan Qin, Chennan Ma, Mian Deng, Zhengzhu Liu, Songzhu Mei, Xinwang Liu, Cheng Wang, and Siqi Shen. The dormant neuron phenomenon in multi-agent reinforcement learning value factorization. In *The Thirty-eighth Annual Conference on Neural Information Processing Systems*.
- David Rolnick, Arun Ahuja, Jonathan Schwarz, Timothy Lillicrap, and Gregory Wayne. Experience replay for continual learning. *Advances in neural information processing systems*, 32, 2019.
- Max Schwarzer, Johan Samir Obando Ceron, Aaron Courville, Marc G Bellemare, Rishabh Agarwal, and Pablo Samuel Castro. Bigger, better, faster: Human-level atari with human-level efficiency. In *International Conference on Machine Learning*, pp. 30365–30380. PMLR, 2023.
- Ghada Sokar, Rishabh Agarwal, Pablo Samuel Castro, and Utku Evci. The dormant neuron phenomenon in deep reinforcement learning. In Andreas Krause, Emma Brunskill, Kyunghyun Cho, Barbara Engelhardt, Sivan Sabato, and Jonathan Scarlett (eds.), *Proceedings of the 40th International Conference on Machine Learning*, volume 202 of *Proceedings of Machine Learning Research*, pp. 32145–32168. PMLR, 23–29 Jul 2023. URL https://proceedings.mlr.press/v202/sokar23a.html.
- Ghada AZN Sokar, Elena Mocanu, Decebal Constantin Mocanu, Mykola Pechenizkiy, and Peter Stone. Dynamic sparse training for deep reinforcement learning (poster). In *Sparsity in Neural Networks: Advancing Understanding and Practice* 2021, 2021.
- Yiqin Tan, Pihe Hu, Ling Pan, Jiatai Huang, and Longbo Huang. Rlx2: Training a sparse deep reinforcement learning model from scratch. *arXiv preprint arXiv:2205.15043*, 2022.
- Yuval Tassa, Yotam Doron, Alistair Muldal, Tom Erez, Yazhe Li, Diego de Las Casas, David Budden, Abbas Abdolmaleki, Josh Merel, Andrew Lefrancq, et al. Deepmind control suite. *arXiv* preprint arXiv:1801.00690, 2018a.
- Yuval Tassa, Yotam Doron, Alistair Muldal, Tom Erez, Yazhe Li, Diego de Las Casas, David Budden, Abbas Abdolmaleki, Josh Merel, Andrew Lefrancq, Timothy Lillicrap, and Martin Riedmiller. Deepmind control suite, 2018b. URL https://arxiv.org/abs/1801.00690.
- Emanuel Todorov, Tom Erez, and Yuval Tassa. Mujoco: A physics engine for model-based control. In 2012 IEEE/RSJ international conference on intelligent robots and systems, pp. 5026–5033. IEEE, 2012.

Wally Welker. Why Does Cerebral Cortex Fissure and Fold?, pp. 3–136. Springer US, Boston, MA, 1990. ISBN 978-1-4615-3824-0. doi: 10.1007/978-1-4615-3824-0\_1. URL https://doi.org/10.1007/978-1-4615-3824-0\_1.

- Guowei Xu, Ruijie Zheng, Yongyuan Liang, Xiyao Wang, Zhecheng Yuan, Tianying Ji, Yu Luo, Xiaoyu Liu, Jiaxin Yuan, Pu Hua, et al. Drm: Mastering visual reinforcement learning through dormant ratio minimization. *arXiv* preprint arXiv:2310.19668, 2023.
- Denis Yarats, Rob Fergus, Alessandro Lazaric, and Lerrel Pinto. Mastering visual continuous control: Improved data-augmented reinforcement learning. In *International Conference on Learning Representations*, 2022. URL https://openreview.net/forum?id=\_SJ-\_yyes8.
- Oleksii Zhelo, Jingwei Zhang, Lei Tai, Ming Liu, and Wolfram Burgard. Curiosity-driven exploration for mapless navigation with deep reinforcement learning. *arXiv* preprint arXiv:1804.00456, 2018.
- Fan Zhou, Chengtai Cao, Ting Zhong, Kunpeng Zhang, Goce Trajcevski, and Ji Geng. Continual graph learning. *ArXiv*, abs/2003.09908, 2020. URL https://api.semanticscholar.org/CorpusID:214612001.

# A RELATED WORK

**Plasticity loss in RL** Recent studies have found that agents guided by the non-stationary objective characteristic of RL suffer catastrophic degradation (Lyle et al., 2023) and ultimately overfit early experiences, which limits their continuous learning ability. This phenomenon is known as plasticity loss. Behaviorally, the loss of plasticity during training can manifest as, for instance, an inability to obtain an effective gradient to guide policy adaptation in fine-tuning (Dohare et al., 2024), limiting potential transfer performance and hard to adapt to new sampling and unseen data (refer to as primacy bias(Nikishin et al., 2022)). While the research on this topic is still in its primary stages, there are several techniques that have been demonstrated to mitigate the loss of plasticity in deep RL. Resetting global networks or dormant neurons (Nikishin et al., 2022; Sokar et al., 2023) and changing activation function (Abbas et al., 2023) are observed to mitigate plasticity loss. Lyle et al. (2024b) empirically find that network normalization particularly layer regularization (LN) can maintain plasticity. Nikishin et al. (2024) introduced copies of random heads for injecting plasticity to improve continual learning ability. PLASTIC (Lee et al., 2023) divides plasticity into input plasticity and label plasticity to deal with them respectively. NaP (Lyle et al., 2024a) alleviates the over-fitting issue from the perspective of the association between regularization and learning rate. In pixel-based deep RL, data augmentation (Ma et al., 2023) and batch size reduction (Obando Ceron et al., 2023) have been analyzed for their effectiveness in reducing plasticity loss. Recent studies have found that mitigating gradient starvation (Dohare et al., 2024), and constraining deviations from initial weights (Kumar et al., 2023; Lewandowski et al., 2024) can also be effective in mitigating plasticity loss. In supervised learning, Lee et al. (2024) proposed to use a combination of fast and slow update networks to balance between fast, fleeting adaptation and slow, steady generalization in supervised learning. Ash & Adams (2020); Berariu et al. (2021) found that both warm initialize and pre-train can better adapt to increasing amounts of data. Our paper proposes a general training schedule from a novel insight about topology growth to effectively help mainstream RL algorithms maintain stable learning while mitigating plasticity loss.

**Pruning in RL** Sokar et al. (2021) showed that training the deep RL policy with a changing topology is difficult due to training instability. Since then, this challenging topic has been well-studied. Policy Pruning and Shrinking (PoPs) (Livne & Cohen, 2020) obtain a sparse deep RL agent with iterative parameter pruning. Graesser et al. (2022); Tan et al. (2022) attempt to train a sparse neural network from scratch without pre-training a dense teacher. Existing methods mainly focus on obtaining a small topology to improve training efficiency. However, our paper explores whether growing the topology from small to large can mitigate the plasticity loss in RL agents rather than training with the maximum number of parameters. In deep RL, the model size commonly utilized is typically small and may encounter policy collapse after scaling up (Schwarzer et al., 2023; Ceron et al., 2024a). Thus, sparse training techniques that have proven beneficial for significantly reducing training costs in fully supervised domains may not yield similar advantages in deep RL in terms of computation cost reduction. Instead, we provide a new perspective and focus on making deep RL agents better use of the growing network size to further improve their learning ability.

# B RELATED PRELIMINARIES

**TD3** In our paper, we use TD3 as a practice backbone for most experiments. Thus, here we introduce the training process of TD3 in detail. TD3 is a deterministic Actor-Critic algorithm. Different from the traditional policy gradient method DDPG, TD3 utilizes two heterogeneous critic networks, i.e.,  $Q_{\theta_{1,2}}$ , to mitigate the over-optimize problem in Q learning.

The training process of TD3 follows the Temporal difference learning (TD):

$$L_Q(\theta_i) = \mathbb{E}_{s,a,s'} \left[ (y - Q_{\theta_i}(s,a))^2 \right] \text{ for } \forall i \in \{1,2\}.$$
(3)

Where  $y=r+\gamma\min_{j=1,2}Q_{\bar{\theta_j}}(s',\pi_{\bar{\phi}}(s')),~p\bar{h}i$  denotes the target network parameters. The actor is updated according to the Deterministic Policy Gradient (Fujimoto et al., 2018):

$$\nabla_{\omega} J(\phi) = \mathbb{E}_s \left[ \nabla_{\pi_{\phi}(s)} Q_{\theta_1}(s, \pi_{\phi}(s)) \nabla_{\phi} \pi_{\phi}(s) \right]. \tag{4}$$

At each training step t, the agent first randomly samples a batch of state transitions from the buffer and calculates the loss gradient as described above. It is worth noting that the proposed method in

our paper is a plug-in and does not affect the training process of the reinforcement learning algorithm itself. For this reason, the training details of the reinforcement learning algorithm are abbreviated in the main text.

**DrQ** DrQ is an algorithm based on maximum entropy reinforcement learning. Its backbone network and training method are the same as SAC (Haarnoja et al., 2018). The soft value function is trained to minimize the squared residual error:

$$J_V(\phi) = \mathbb{E}_s 1/2(V_\phi(s) - Q_\theta(s, a) + \log \pi_\psi(a|s)) \tag{5}$$

where a are sampled according to the current policy, instead of the replay buffer. The soft Q-function parameters can be trained to minimize the soft Bellman residual:  $J_Q(\theta) = \mathbb{E}_{s,a} \sim D[\frac{1}{2}(Q_{\theta}(s,a) - \hat{Q}(s,a))^2]$ . Then the policy network can be learned by directly minimizing the expected KL divergence

$$J(\psi) = \mathbb{E}_{s \sim D}[D_{KL}(\pi_{\phi}(\cdot|s)||\frac{\exp Q(s)}{Z(s)})]$$
(6)

## C EXPERIMENTAL DETAILS

#### C.1 Network Structure

**TD3** The normal size of the TD3 network we used is the official architecture, and the detailed setting is shown in Tab 1. Besides, the network we used for Scale-up experiments incrementally adds the depth of both the actor and critic. For The 1.8x agent, we add one MLP as a hidden layer in two critic networks in front of the output head and one MLP layer as the embedding layer at the front of the actor. And the hidden dim is also increased to 256. And so on, we follow the above approach to grow the model by an equal amount each time.

Layer	Actor Network	Critic Network
Fully Connected	(state dim, 256)	(state dim, 256)
Activation	ReLU	ReLU
Fully Connected	(256, 128)	(256, 128)
Activation	ReLU	ReLU
Fully Connected	(128, action dim) and (128, 1)	
Activation	Tanh	None

Table 1: Network Structures for TD3

**DrQ** We use DrQ to conduct experiments on robot control tasks within DeepMind Control using image input as the observation. All experiments are based on previously superior DrQ algorithms and maintain the architecture from the official setting unchanged.

#### C.2 Hyperparameter

TD3 Our codes are implemented with Python 3.8 and Torch 1.12.1. All experiments were run on NVIDIA GeForce GTX 3090 GPUs. Each single training trial ranges from 6 hours to 21 hours, depending on the algorithms and environments, e.g. DrQ spends more time than TD3 to handle the image input and DMC needs more time than OpenAI mujoco for rendering. Our TD3 is implemented with reference to github.com/sfujim/TD3 (TD3 source-code). The hyper-parameters for TD3 are presented in Table 2. Notably, for all OpenAI mujoco experiments, we use the raw state and reward from the environment and no normalization or scaling is used. An exploration noise sampled from N(0,0.1) (Lillicrap, 2015) is added to all baseline methods when selecting an action. The discounted factor is 0.99 and we use Adam Optimizer (Kingma, 2014) for all algorithms. Tab.2 shows the common hyperparameters of TD3 used in all our experiments. And for NE, following the related work (Elsayed et al., 2024), we use L2 weight clipping on dormant neurons that are already reset and pruned from the current topology. We apply this technique consistently across all compared methods to ensure a fair comparison. Additionally, we introduce layer normalization after the hidden layers of both the critic and actor networks to establish the LN-TD3

baseline for comparison. Notably, other methods do not incorporate normalization mechanisms to ensure a fair comparison. We reproduce Plasticity Injection Following the guidelines from the official paper (Nikishin et al., 2024). We utilize the default settings of the official ReDo codebase for our comparative analysis https://github.com/google/dopamine/tree/master/dopamine/labs/redo. For Reset-TD3, after a lot of empirical debugging, we found that parameter reset every 90,000 step is a generally better setting, and fixed it as a hyperparameter. We use seeds 0 to 14 for all the experiments. We suggest using seed 5 to reproduce the HalfCheeetah learning curve in the main text.

Hyperparameter	NE-TD3	Reset-TD3	ReDo-TD3	LN-TD3	PI-TD3	
Actor Learning Rate	$1e^{-4}$	$1e^{-4}$	$1e^{-4}$	$1e^{-4}$	$1e^{-4}$	$1e^{-4}$
Critic Learning Rate	$1e^{-3}$	$1e^{-3}$	$1e^{-3}$	$3e^{-4}$	$3e^{-4}$	$1e^{-3}$
Representation Model Learning Rate	None	None	None	$1e^{-4}$	$5e^{-3}$	$5e^{-3}$
Discount Factor	0.99	0.99	0.99	0.99	0.99	0.99
Batch Size	128	128	128	128	128	128
Buffer Size	1e6	1e6	1e6	1e6	1e6	1e6

Table 2: A comparison of common hyperparameter choices of algorithms. We use 'None' to denote the 'not applicable' situation.

**DrQ** We use DrQ as the backbone to verify our methods on DeepMind Control tasks. And All the methods use the same setting. The details can be seen in Tab.3. Notably, For Reset-DrQ, we only reset the last three MLP layers which is suggested by their paper.

Hyperparameter	NE-DrQ	Reset-DrQ	ReDo-DrQ	LN-DrQ	PI-DrQ	
Replay buffer capacity	1e6	1e6	1e6	1e6	1e6	1e6
Action repeat	2	2	2	2	2	2
Seed frames	4000	4000	4000	4000	4000	4000
Exploration steps	2000	2000	2000	2000	2000	2000
n-step returns	3	3	3	3	3	3
Mini-batch size	256	256	256	256	256	256
Discount $\gamma$	0.99	0.99	0.99	0.99	0.99	0.99
Optimizer	Adam	Adam	Adam	Adam	Adam	Adam
Learning rate	1e - 4	1e - 4	1e - 4	1e - 4	1e - 4	1e-4
Agent update frequency	2	2	2	2	2	2
Critic Q-function soft-update rate	0.01	0.01	0.01	0.01	0.01	0.01
Features dim.	50	50	50	50	50	50
Hidden dim.	1024	1024	1024	1024	1024	1024

Table 3: A default set of hyper-parameters used in our DrQ based methods.

NE For Humanoid and Ant tasks, we set grow interval  $\Delta T=25000$ , grow number k=0.01\* rest capacity, Prune upper bond  $\omega=0.4$ , ending step is the max training step, the threshold of ER is 0.35 and the decay weight  $\alpha=0.02$ (which is used in all the tasks). For other OpenAI Mujoco tasks, we set grow interval  $\Delta T=20000$ , grow number k=0.15\* rest capacity, Prune upper bond  $\omega=0.2$ , ending step is the max training step, the threshold of ER is 0.25. Notably, as for the continuous adaptation tasks, we set  $\Delta T=50000$  to ensure the topology can continue growing during the long-term training, and other parameters are same as Humanoid. When we combine our method with DrQ, We use single set of hyperparameters to apply on all four tasks.  $\Delta T$  is set as 20000 to ensure the network can grow quickly to handle the complex input. The grow number k is 0.02\* rest capacity for critic and 0.01\* rest capacity for actor. The Prune upper bond  $\omega=0.23$  and the threshold of ER is 0.18. We set ER step C to 450 for Mujoco tasks and 150,250 is work on DMC.

# D PSEUDOCODE CODE

#### D.1 PSEUDO-CODE FOR NE

# Algorithm 1 Neuroplastic Expansion TD3

```
\pi_{\phi}: All parameters in actor. Q_{\theta_{\{1,2\}}}: All parameters in critics, M_l: Sparse mask in layer l. Initial sparse rate Sp # Initialize the sparse networks for stable starting keep \theta^{l \in \{1,N\}}, \phi^{l \in \{1,N\}} dense, \theta^{l \in 1,N}. \theta, \phi \leftarrow \operatorname{Erdos-Renyi}(Sp)
```

## Train the RL policy

```
\begin{aligned} a &\leftarrow \pi_{\check{\phi}}(s) \text{ (with Gaussian noise)} \\ \text{Observe } r \text{ and new state } s' \\ \text{Fill } D \text{ with } (s, a, r, s') \\ \text{\# Experience review} \\ \text{if } random(0, 1) &> \Delta f(\theta) \text{ then} \\ \text{sample a batch from bottom } \frac{1}{4}D \\ \text{else} \\ \text{sample a batch from total } D \\ \text{end if} \\ \text{Update } Q_{\check{\theta}_{\{1,2\}}}, \pi_{\check{\phi}} \text{ based on TD3} \end{aligned}
```

# D.2 PSEUDO-CODE FOR CONTROLLING THE PRUNING SIZE BASED ON THE CLIP FUNCTION

# Algorithm 2 Control pruning size

972

973 974

975 976

977

978

979

980

981

982

983

984

985

986

987

988

990

991

992

993

994

995 996 997

998 999

1000

1001

1002

1003

1005

1007

1008 1009 1010

1011 1012

1013 1014

1015

1016

1017

1018

1019

1020 1021

1023

1024

1025

```
1: Input:
 2: # Enter the necessary inputs required by the Clip function Clip(min value, size of pruning set,
     max value)
        min value: min pruning threshold (set to be 0)
        |\mathbb{I}^l_{prune}|: the size of the pruning set \mathbb{I}^l_{prune}
 5:
        |\mathbb{I}_{qrow}^l|: the size of the growth set \mathbb{I}_{qrow}^l
 6:
        \omega: a preset ratio in [0,1)
        # max \ value = \omega \times |\mathbb{I}_{grow}^l|: max pruning amount
 7:
 8: Output: Constrained pruning size
 9:
10: if |\mathbb{I}_{prune}^l| < min \ value \ \mathbf{then}
11:
          Return min value
12:
          # This branch is not reached since we set min value to be 0
13: else if min \leq |\mathbb{I}_{prune}^l| \leq \omega \times |\mathbb{I}_{qrow}^l| then
          Return |\mathbb{I}^l_{prune}| # Original size retained if within limit
14:
15:
16: else if |\mathbb{I}^{l^{\circ}}_{prune}| > \omega \times |\mathbb{I}^{l}_{grow}| (max value) then
          Return max value
17:
          # Will randomly remove excess elements from the pruning set \mathbb{I}^l_{prune} then
18:
19: end if
```

#### E DETAILED EXPLANATION OF THE GROWTH MECHANISM

We follow the classical sparse network exploration method in (Evci et al., 2020). We use all the weights to calculate the gradient backpropagation because we want to find a weight subgraph composed of multiple candidates to add to the current network, that is, the newly added weight subsets jointly obtain high gradient magnitude under the influence of each other, and calculating the weights one by one will ignore the interaction between them and other weights in the subset, resulting in serious errors and high-cost computation. To this end, we compute the full weight to cheaply select the valid subgraphs. However, this evaluation does introduce errors that add low-quality weights, and the reason why this growth framework is effective is we hypotheses that real-time pruning removes the error caused by growth by pruning the low-quality neurons in time. In the future, we will further optimize the growth mechanism to improve the accuracy of its evaluation.

#### F ADDITIONAL EXPERIMENTS

#### F.1 ORTHOGONAL EXPERIMENT

We use our method in combination with other mainstream plasticity loss mitigation methods on two mujoco tasks to further verify whether our method has the potential ability to improve the performance of other techniques. Specifically, we combine NE with layer normalization, ReDo, and reset to verify whether topology growth can improve existing techniques. As shown in Figure 11, results illustrate that NE has obvious orthogonal gains with well-performing baselines. In particular, resetting and ReDO empirically perform much better when combined with our method. 7 runs for each method, and we use the NE score as the normalized performance.

#### F.2 Analysis of Grow & Rrune Rate

We conducted ablation experiments on dormant neuron pruning across two intricate tasks in Tab.4. The findings demonstrate the significant and generalized benefits of dormant neuron pruning for our framework.

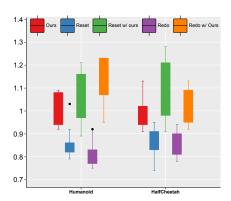


Figure 11: Quadrature gain of our method combined with the baselines, with each method executed using seven independent seeds.

Method	Cartpole Swingup Sparse	Walker Walk
w/ prune	$425.09 \pm 45.28$	$491.28 \pm 40.62$
w/o prune	$382.14.28 \pm 29.86$	$367.51.24 \pm 43.06$

Table 4: Performance (Average of 10 runs).

### F.3 ANALYSIS OF GROW & RRUNE RATE

In table.5, we set experiments concerning growth rate and pruning rate. Our method shows good performance on both image-based and state-based tasks with a slow growth schedule, i.e.  $0.001 \sim 0.009$ , but it is not sensitive to cropping rate, i.e., keeping it between 10% and 40%

Task	0.0005	0.00010	0.00050	0.00100	0.00150
state-input (Ant)	$7529.15 \pm 132.36$	$7749.25 \pm 127.73$	$7714.28 \pm 147.56$	$7308.47 \pm 261.95$	$7287.39 \pm 384.02$
image-input (DMC Reacher Hard)	$416.72 \pm 50.37$	$442.31 \pm 56.42$	$475.46 \pm 34.11$	$431.74 \pm 52.09$	$419.38 \pm 37.24$

Table 5: The evaluations of growth rate on vector-input and image-input tasks. Average of 3 runs.

#### F.4 ANALYSIS OF STARTING SPARSITY RATE

We empirically find that starting from around 0.25 is a general and effective setting for growth. For the cycle adaptation task we find that starting from 0.15 is a good choice. In the future, we will explore how to find the appropriate sparsity adaptively according to the task.

We uniformly sample different starting sparsity rates and test the performance. In table 6, we find that the effect is similar when the sparsity ratio is between [0.7, 0.8], too sparse network cannot learn efficiently in the early stage of training, and too dense network will limit the gain brought by network growth. Therefore, we set it to 0.75 uniformly.

Task	0.85	0.8	0.75	0.7	0.65
state-input (Ant)	$6962.52 \pm 297.41$	$7694.37 \pm 115.28$	$7749.25 \pm 127.73$	$7681.61 \pm 108.07$	$7255.34 \pm 212.86$
image-input (DMC Reacher Hard)	$425.95 \pm 27.62$	$480.73 \pm 35.18$	$475.46 \pm 34.11$	$492.13 \pm 22.53$	$432.67 \pm 29.17$

Table 6: The evaluations of initial sparsity on vector-input and image-input tasks. Average of 3 runs.

#### F.5 VERIFY THE EFFICIENCY OF EXPERIENCE REVIEWER

The experience replay module is related to reducing forgetting in the later training stage and enhancing stability-plasticity ability. The experiment depicted in Fig. 7a illustrates that frequent alterations to the network topology can induce sudden shifts in network computations, and may prune neurons holding valuable information, leading to instability in subsequent training phases. The trajectory visualization (Figure 4) demonstrates that the agent may exhibit suboptimal behavior by forgetting the initial skill (standing up). Consequently, we introduce the experience replay mechanism during the later stages of training to prompt the network to revisit earlier data, mitigating forgetting and fostering stability in the latter training phases.

To further authenticate the efficacy of empirical replay (ER) across a spectrum of tasks, we focus on four challenging image input tasks: Reacher Hard and Walker Walk in DMC, along with two sparse reward manipulator control tasks: Hammer (sparse) and Sweep Into (sparse) in Metaworld. The results in Table.7 shows reveal enhanced performance and notably reduced variance following the integration of the experience replay mechanism. This outcome underscores that experience replay fosters training stability.

Method	Reacher Hard	Walker Walk	Hammer sparse (success rate)	Sweep Into sparse (success rate)
NE w/ ER	$475.46 \pm 34.11$	$491.28 \pm 40.62$	$0.54 \pm 0.13$	$0.61 \pm 0.09$
NE w/o ER	$419.25 \pm 65.73$	$427.31 \pm 73.84$	$0.47 \pm 0.21$	$0.52 \pm 0.16$

Table 7: The evaluations of initial sparsity on vector-input and image-input tasks. Average of 3 runs.

In addition, we set a study of experience review (ER) on various tasks in Tab.8-10, and the results show that without ER, although all the agents with different seeds can learn efficiently in the early stage, the performance will drop at the later training stage and become unstable in some runs(high std). We also find that this phenomenon is more pronounced on complex sparse reward tasks as well as image input scenarios. Therefore we suggest employing ER in complex tasks to assist our method for stable training.

Method	at $1/2$ training stage	at $3/4$ training stage	end of training
NE w/ ER	$6635.12 \pm 245.28$	$7258.18 \pm 151.66$	$7749.25 \pm 127.73$
NE w/o ER	$6673.54 \pm 216.41$	$6896.92 \pm 264.23$	$7235.14 \pm 493.83$

Table 8: Performance on vector-input task (Ant) (Average of 10 seeds).

Method	at $1/2$ training stage	at $3/4$ training stage	end of training
NE w/ ER	$408.22 \pm 74.14$	$462.09 \pm 48.74$	$475.46 \pm 34.11$
NE w/o ER	$413.75 \pm 79.22$	$439.02 \pm 86.15$	$419.25 \pm 65.73$

Table 9: Performance on image-input task (Reacher Hard) (Average of 10 seeds).

Method	at $1/2$ training stage	at $3/4$ training stage	end of training
NE w/ ER	$396.69 \pm 83.27$	$416.39 \pm 55.26$	$424.76 \pm 47.68$
NE w/o ER	$397.15 \pm 79.22$	$421.02 \pm 61.08$	$402.88 \pm 71.23$

Table 10: Performance on sparse reward task (Cartpole Swingup Sparse)(Average of 10 seeds).

### F.6 ANALYSIS OF GROW MODE

The choice of the control mode concerning the topology growth is empirical and we have tested several modes in the experimental phase, i.e Uniform schedule, warm decay, and cosine annealing. We show the previous comparison in Table 11, the results show that although all modes are efficient, cosine annealing performs the best. We guess that this is because it includes cyclicality on the basis of warm decay, which is more robust in practice.

Mode	Cartpole Swingup Sparse
Cosine annealing	$425.09 \pm 45.28$
Uniform	$389.66 \pm 41.53$
warm decay	$392.24 \pm 31.95$

Table 11: The evaluations of growth mode on vector-input and image-input tasks. Average of 5 runs.

#### F.7 THE RATE OF DECREASE IN ACTIVATED NEURON NUMBERS

We have included Tab.12 to explicitly display the rate of decrease in activated neuron numbers (percentage decrease at each step) during training. In our comparison with vanilla TD3, NE slows down the decrease in activated neurons by approximately 50% compared to vanilla TD3. stability.

Method	Humanoid $(10^{-6})$	$Ant(10^{-6})$	HalfCheetah $(10^{-6})$
NE + TD3 Vanilla TD3	$5.43 \pm 0.71$ $9.81 \pm 0.463$	$4.95 \pm 0.28$ $7.06 \pm 0.54$	$6.36 \pm 0.18$ $0.47 \pm 0.21$
$11.61 \pm 0.19$			

Table 12: The evaluations of initial sparsity on vector-input and image-input tasks. Average of 3 runs.

#### F.8 VISUALIZATION OF THE NETWORKS WITH LOW ACTIVATED NEURON RATIO

When the activated neurons ratio is low, means the networks contain lots of dormant (dead) neurons that retain useless (negative) weights. In this section, we add two visualizations to demonstrate the detrimental effects of accumulating lots of dormant neurons in a network: it diminishes the network's overall representational capacity during training and leads to suboptimal policy.

We contrasted the backpropagation gradient heatmaps of a standard network with those of a network containing numerous dormant neurons (Figure 12), where darker colors indicate higher gradients and faster weight optimization. Both networks use the same data for input. The findings indicate that when a network harbors a substantial number of dormant neurons, the gradient guidance is notably diminished, thereby constraining the learning efficacy. This limitation stems from dormant neurons being unable to trigger the activation function, rendering them unseen on the computational graph and impeding the backflow of gradients.

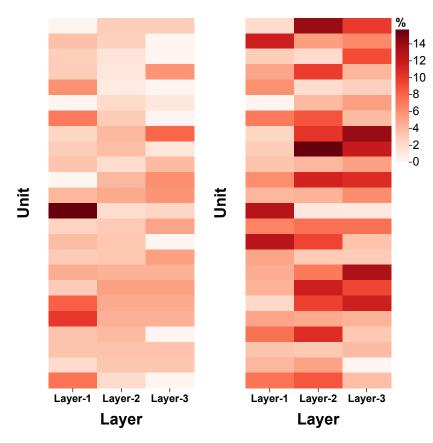


Figure 12: Heat map. Darker colors indicate higher gradients and faster weight optimization. Both networks use the same data for input.

We compare the behaviors of the regular policy and the policy featuring numerous dormant neurons in Figure 13, it becomes evident that the latter tends to exhibit suboptimal behavior due to its reduced learning capacity.

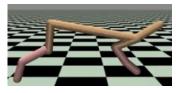
# Dormant neuron: Although moving, fail to learn the desired running skills







## Activated neuron: Achieve smooth running







Behavior after Policy training

Figure 13: Compare of the behaviors after training.

## F.9 ABLATION STUDY OF REPLAY RATIO

We test the effect of different Replay Ratio (RR) on all four DMC tasks. The results in Figure 14 show that with the increase of RR, the performance of baseline and NE increased slightly (the effect of our method was more obvious). We concluded that this was because changing RR proved to be an effective way to alleviate plasticity loss in VRL (Ma et al., 2023).

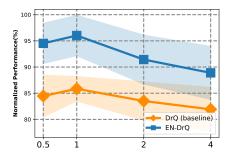


Figure 14: Analysis of different Replay Ratio.

## F.10 Detail Results of Different Network Size

Figure 15 shows the results for uniform fine-grained size sampling.

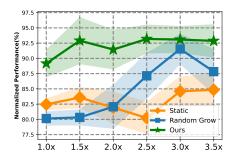


Figure 15: Performance comparison for different final model sizes.